

The Pedersen current carried by electrons: a non-linear response of the ionosphere to magnetospheric forcing

S. C. Buchert¹, T. Tsuda², R. Fujii², and S. Nozawa²

¹Swedish Institute of Space Physics, Uppsala, Sweden

²Solar-Terrestrial Environment Laboratory, Nagoya University, Japan

Received: 3 January 2008 – Revised: 18 June 2008 – Accepted: 7 August 2008 – Published: 22 September 2008

Abstract. Observations by the EISCAT Svalbard radar show that electron temperatures T_e in the cusp electrojet reach up to about 4000 K. The heat is tapped and converted from plasma convection in the near Earth space by a Pedersen current that is carried by electrons due to the presence of irregularities and their demagnetising effect. The heat is transferred to the neutral gas by collisions. In order to enhance T_e to such high temperatures the maximally possible dissipation at 50% demagnetisation must nearly be reached. The effective Pedersen conductances are found to be enhanced by up to 60% compared to classical values. Conductivities and conductances respond significantly to variations of the electric field strength E , and “Ohm’s law” for the ionosphere becomes non-linear for large E .

Keywords. Ionosphere (Electric fields and currents; Ionosphere-magnetosphere interactions; Ionospheric irregularities)

1 Introduction

When an electric field \mathbf{E}_\perp perpendicular to the magnetic field \mathbf{B} is applied in the ionosphere by plasma convection,

$$\mathbf{E}_\perp = -\mathbf{v}_\perp \times \mathbf{B}, \quad (1)$$

\mathbf{v}_\perp is the unmagnetized plasma velocity, then a current flows perpendicular to \mathbf{B} , $\mathbf{j}_\perp = \sigma_P \mathbf{E}_\perp - \sigma_H \mathbf{E}_\perp \times \mathbf{B} / B$. σ_P and σ_H are the Pedersen and Hall conductivities, respectively. This is Ohm’s law for the ionosphere.

According to http://en.wikipedia.org/wiki/Ohm's_law “Ohm’s law states that, in an electrical circuit, the current passing through a conductor between two points is directly

Correspondence to: S. C. Buchert
(scb@irfu.se)

proportional to the potential difference.” This implies that σ_P and σ_H should be independent of \mathbf{E}_\perp . Indeed, expressions for σ_P and σ_H derived in text books and papers (e.g. Brekke and Hall, 1988; Kelley, 1989, Chapter 2.2) show that the conductivities depend mainly on the local electron density, and slightly on parameters of the neutral atmosphere, like density and composition, affecting the ion-neutral and electron-neutral collision frequencies as well as on the strength of the geomagnetic field which is rather constant in time, but varies somewhat over geographic position. The standard expressions for σ_P and σ_H do not contain explicitly the electric field. If they did, one might say that Ohm’s law would not be valid in the ionosphere.

In the auroral and equatorial electrojets $|\mathbf{E}_\perp|$ can become so large that the velocity difference between the unmagnetized ions and the magnetized electrons exceeds the ion sound velocity. The Farley-Buneman instability gets excited (Farley, 1963) when the convection electric field increases above a threshold of about 22 mVm^{-1} , E_{th} . Incoherent scatter radar measurements have shown that in the auroral electrojet the electron temperature, T_e rises with increasing $|\mathbf{E}_\perp|$, if $|\mathbf{E}_\perp| > E_{th}$ (Schlegel and St.-Maurice, 1981; Jones et al., 1991). This increase of T_e has a small effect on σ_P and σ_H .

Haldoupis (1994) compared the directions of phase velocities of irregularities and the EISCAT $\mathbf{E} \times \mathbf{B}$ flow direction measured in the F region. He attributed the differences to a weak demagnetisation of the electrons. Zhang et al. (2004) simulated the effects of an electric field on the ionosphere. They also included an anomalous collision frequency, obtained from microphysical considerations (Sudan, 1983) and the heating formula by Robinson (1986), in the calculation of the effective conductivities.

Buchert et al. (2006) showed that electrojet irregularities affect directly the mean current (DC), $\langle \mathbf{j} \rangle$, which is averaged over spatial and temporal scales that are large compared to those of the irregularities. When warmer electrons collide

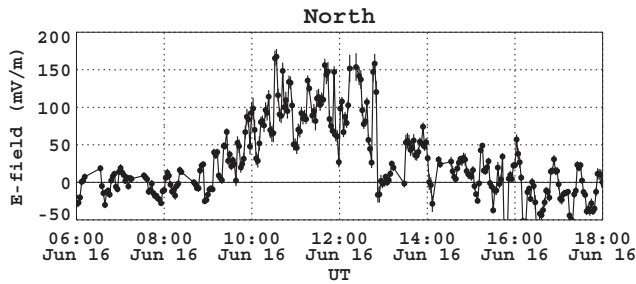


Fig. 1. Electric field along geographic north estimated from the CP2 cycled antenna positions of the ESR.

(mainly inelastically) with neutral molecules, then power is converted into heat and transferred to the neutral gas. Since the unmagnetized ions are practically frozen into the neutral gas and do not contribute much to dissipation, the power transfer is achieved by a Pedersen current j_P carried by electrons. j_P closes field-aligned current, causing a divergence of the downward field-aligned Poynting flux, and it taps power from the free energy reservoir of plasma convection in the huge near Earth space. Buchert et al. (2006) expected that this would have a much larger effect on the effective conductivities than the increase of T_e . But how strongly the effective σ_P and σ_H would change in response to increasing $|E_\perp|$ and to the corresponding excitation of irregularities, remained unclear to some extent.

In this work we derive from experimental data, that at times significant dissipation in the electrojet region is caused by irregularities and therewith the effective Pedersen conductivity responds promptly to changes of E_\perp whenever $|E_\perp|$ is high. The load of the complete ionospheric layer on magnetospheric convection may be parameterized by integrating along the magnetic field:

$$\Sigma_P = \int dz \sigma_P, \quad (2)$$

where z is a coordinate along B , approximately the height at high latitudes. We also address the question how much the integrated Pedersen conductivity, i.e. the conductance Σ_P , is affected by the irregularity enhanced σ_P in the electrojet layer.

2 Observations

The data were recorded by the EISCAT Svalbard incoherent scatter radar (ESR) on 16 June 2005. The radar has a dish of 42 m diameter with fixed pointing along the geomagnetic field at 300 km altitude, and a steerable dish of 32 m diameter. The transmitter power goes for a few seconds long time intervals alternating to the 42 m or the 32 m dishes. The raw signal correlations need to be integrated over 2–3 min before

the standard incoherent scatter data fitting can be applied successfully, and so along B the analysis of N_e , T_e , and the ion temperature T_i is over time intervals of this length normally joining each other. The 32 m dish cycles over three pointing directions, the total cycle taking about 6.5 min. This is called the CP2 mode for the ESR. From the observed line-of-sight velocities along these different pointing directions E_\perp is estimated. We need to assume that E_\perp and v_\perp are constant over the 32 m antenna cycle, ≈ 6.5 min, as well as homogeneous over an area of roughly 100 km across.

Strong electric fields are seen over about 4 h, from 09:00 until 13:00 UT, the time period that we are focusing on. Figure 1 shows the dominant component of E . The standard fitting of incoherent scatter theory to the signal correlations gives the electron density N_e , T_e , and the ion temperature T_i along a profile following the field-aligned direction of the 42 m antenna. Results of the fits in the E region height range are displayed in Fig. 2. T_e is clearly enhanced in the lower E region when also the electric field is high, compare with Fig. 1. T_e reaches up to about 4000 K, which is about twice the value found in previous studies of E region electron heating (Jones et al., 1991). This seems to be a very high temperature, and so is T_i at the same time in the upper E region where partially unmagnetized ions get heated by friction with the neutral gas. Bahcivan (2007) obtained similarly high values for T_e with the Sondrestrom incoherent scatter radar. These and our observations were made at a location and local time, where and when typically the cusp is found, i.e. the footprint of field-lines that have been opened by magnetic reconnection on the dayside. In the cusp possibly larger electric fields and stronger electron heating occur than in the auroral zone where the observations by Jones et al. (1991) had been made.

2.1 Analysis

The effective Pedersen conductivity of the ionosphere is found by equating the Ohmic dissipation with the thermal power transferred from the warmer electrons to the neutral gas. From the viewpoint of the electrons this is the cooling rate. Models for the rates due to different reactions are summarized by Schunk and Nagy (2000, Chapter 9.7). We take into account rotational and vibrational excitations of the N_2 and O_2 molecules, fine structure excitation of the O atom, and elastic collisions with N_2 , O_2 , and O. Input is T_e , observed by the ESR, and the neutral density, composition and temperature calculated with the MSIS model (Hedin, 1991, <http://modelweb.gsfc.nasa.gov/atmos/msise.html>) using the relevant values of solar flux and magnetic activity index. Output is the cooling rate per electron $l_e(T_e - T_n, n_{N_2}, n_{O_2}, n_O)$, where T_n denotes neutral temperature, and n_{N_2} , n_{O_2} , and n_O number densities of N_2 , O_2 and O, respectively.

Ohmic dissipation in the presence of irregularities is equal to the mean current times the electric field applied by

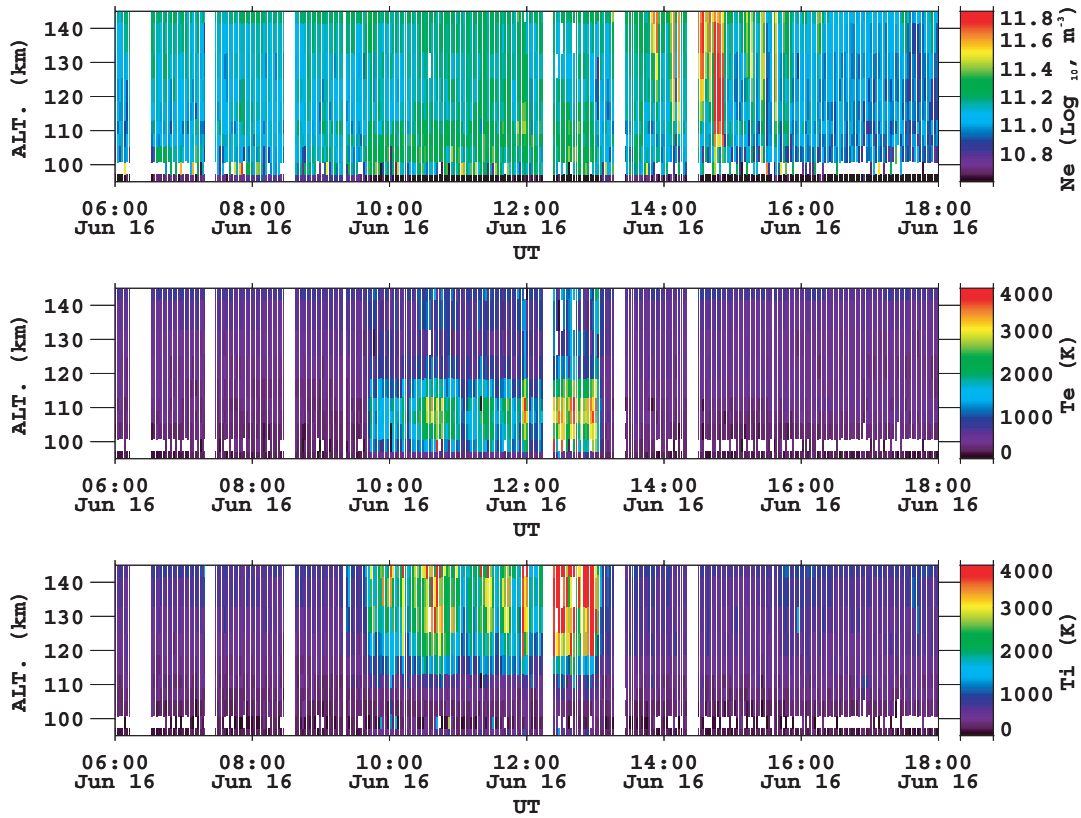


Fig. 2. Colour coded N_e , T_e , and T_i over altitude and UT.

magnetospheric convection, $\mathbf{E}_{\perp,0} \cdot \langle \mathbf{j} \rangle$. The dissipation and generation of electromagnetic power by fields and currents of the irregularities themselves do on average out to zero (Buchert et al., 2006). Because only the mean current and velocities are needed here, we omit from now on the $\langle \rangle$ brackets. Electrons are heated by the electron current $-n_e e \mathbf{v}_e$, ions by the ion current $n_e e \mathbf{v}_i$, where $\mathbf{v}_{e,i}$ are the mean (fluid) velocities of electrons and ions.

The effect of irregularities on the DC and mean velocities is parameterized by an anomalous collision frequency ν^* between electrons and ions. In many previous works values for ν^* were estimated by assuming specific properties of the irregularities, namely that their phase velocity is equal to the sound velocity (Sudan, 1983). Here we use experimental data instead.

To describe this method we start with the mean velocities fulfilling the stationary momentum equations per particle for electrons and ions perpendicular to \mathbf{B} :

$$-e(\mathbf{E} + \mathbf{v}_e \times \mathbf{B}) = m_e \nu_{en} (\mathbf{v}_e - \mathbf{u}) + m_e \nu^* (\mathbf{v}_e - \mathbf{v}_i) \quad (3)$$

$$e(\mathbf{E} + \mathbf{v}_i \times \mathbf{B}) = m_i \nu_{in} (\mathbf{v}_i - \mathbf{u}) + m_e \nu^* (\mathbf{v}_i - \mathbf{v}_e). \quad (4)$$

$m_{i,e}$ are the ion and electron masses, $\nu_{i,en}$ the collision frequencies of ions and electrons with neutral particles, respectively. \mathbf{u} is the velocity of the neutral gas, which we assume

to be zero. The subscripts \perp at \mathbf{E} and velocities have been omitted, because only the plane perpendicular to \mathbf{B} is considered.

Summing the anomalous terms in Eqs. (3) and (4) verifies that the irregularities effectively exchange momentum between ions and electrons, but no extra external momentum is involved by this. Ions and electrons also exchange momentum by Coulomb collisions which should be added to ν^* , but their effect is negligible compared to ν_{en} . Solving Eqs. (3) and (4) for \mathbf{v}_e and \mathbf{v}_i gives quite cumbersome expressions.

To simplify we neglect firstly the effect of electron-neutral collisions on the electron momentum, because $\nu_{en} \ll \Omega_e$ at the relevant altitudes (100–112 km), and secondly the effect of the anomalous term with ν^* in the ion momentum balance, because the electron mass is so small compared to m_i . $\Omega_{e,i} = eB/m_{e,i}$ are the gyro frequencies of electrons and ions, respectively, and the ratios of gyro to collision frequencies are $\kappa_i = \Omega_i/\nu_{in}$ and $\kappa^* = \Omega_e/\nu^*$. These are calculated using the IGRF and MSIS. Solving now for the velocities gives

$$\mathbf{v}_i = \frac{\kappa_i}{1 + \kappa_i^2} \frac{\mathbf{E}}{B} + \frac{\kappa_i^2}{1 + \kappa_i^2} \frac{\mathbf{E} \times \mathbf{B}}{B^2}, \quad (5)$$

$$\mathbf{v}_e = -\frac{\kappa^*}{1 + (\kappa^*)^2} \frac{\mathbf{E}'}{B} + \frac{(\kappa^*)^2}{1 + (\kappa^*)^2} \frac{\mathbf{E}' \times \mathbf{B}}{B^2}, \quad (6)$$

where $\mathbf{E}' = \mathbf{E} + \mathbf{v}_i \times \mathbf{B}$ is the electric field in the reference frame of the ions. Its magnitude E' is only slightly less than that of the observed E :

$$E'^2 = \frac{1}{1 + \kappa_i^2} E^2, \quad (7)$$

because $\kappa_i \ll 1$ at the relevant altitudes. Dissipation by the electron Pedersen current is obtained by multiplying Eq. (6) with $-e\mathbf{E}'$, and the result must be equal to the cooling rate:

$$l_e = -e\mathbf{v}_e \cdot \mathbf{E}' = e \frac{\kappa^*}{1 + (\kappa^*)^2} \frac{E'^2}{B} = \frac{\sigma_P^*}{N_e} E'^2 \quad (8)$$

In Eq. (8) we have introduced the anomalous Pedersen conductivity $\sigma_P^* = N_e l_e / E'^2$, which can be estimated from our data: N_e , l_e and E'^2 are derived directly from ESR observations using the model electron cooling rates of Schunk and Nagy (2000, Chapter 9.7) and Eq. (7).

The “demagnetisation” ratio κ^* is obtained from the left part of Eq. (8). The solutions are

$$\kappa^* = \frac{A}{2} \pm \sqrt{\frac{A^2}{4} - 1} \quad (9)$$

where $A = e(E')^2 / Bl_e$. For $A > 2$ there are two real positive solutions for κ^* . The larger one, $\kappa^* > 1$, corresponds to a weaker demagnetization of the electrons, and the angle between the mean electron velocity and the $\mathbf{E} \times \mathbf{B}$ direction is less than 45° . We do not adopt the smaller of the solutions $\kappa^* < 1$ which would correspond to a smaller (less unstable) velocity difference between ions and electrons.

For $A < 2$ the solutions for κ^* become complex, which is unphysical. In order to sustain a certain cooling rate l_e , the electric field in the reference frame of the ions must have a minimum strength, $E' \geq \sqrt{Bl_e/e}$. This result of our analysis is possibly relevant for microspherical studies of the irregularities.

When estimating σ_P^* from our data, sometimes extremely high values were obtained, and κ^* turned out to be complex. In order to explain this, we made scatter plots of the observed T_e over E . Compared with the corresponding plots published by Jones et al. (1991) ours showed data points with a high T_e and relatively low E , particularly in the time periods 09:40–09:50 UT and 12:40–13:10 UT. These data would give complex, unphysical values for κ^* .

Why this happens we explain by the way the electric fields are measured at the ESR with the CP2 scan. Higher perpendicular electric fields occur statistically less frequently than lower fields. If there is strong E in some area, E in the surrounding areas is more likely lower than higher. When the field-aligned antenna of the ESR observes high T_e due to strong E , the movable antenna observes at locations roughly ~ 100 km away, where statistically E is lower. Therefore E gets rather under- than overestimated. When the only moderately enhanced T_e is observed at the field-aligned position,

and an area with high E is observed in one or more of the scan positions, then also overestimation of E can happen, but statistically this happens less frequently. Thus the E estimates tend to be biased towards underestimation increasingly for increasing E . Jones et al. (1991) had used the tristatic UHF radar where this problem does not occur, because E is measured on the same magnetic field line as T_e .

In order to obtain plausible values of σ_P^* even when E from the ESR 32 m data seems to be an underestimation, we assume that the real E' is close to $\sqrt{Bl_e/e}$. So complex κ^* values are replaced by $\kappa^* = 1$, and a correspondingly corrected σ_P^* is calculated. Our assumptions also imply that the demagnetisation of the electrons by irregularities gets never so strong that the angle between \mathbf{v}_e and the $\mathbf{E} \times \mathbf{B}$ direction exceeds 45° .

2.2 Results

Profiles of temperatures, Pedersen conductivities, and collision frequencies are shown in Fig. 3 for a case of relatively moderate electron heating ($T_e \approx 1500$ K or less) and of extremely strong heating, T_e up to about 4000 K. As expected, the effect of enhanced T_e on the electron-neutral collision frequency and on the Pedersen conductivity is always small compared to the anomalous effect. For the high T_e case σ_P^* estimated according to $N_e l_e / E'^2$ becomes extremely large, the red area extending beyond the borders of the plot. As described in the previous section, such high σ_P^* would be impossible to explain with any real \mathbf{v}_e fulfilling Eq. (6). Certainly estimating E' from different widely spaced ESR 32 m measurements gives a too low value in this case, only about 30 mVm^{-1} . If we set instead $E' = \sqrt{Bl_e/e}$, more reasonable values of $100\text{--}130 \text{ mVm}^{-1}$ are obtained, depending on the altitude, and also the corrected profile of $\sigma_P + \sigma_P^*$ shown by the black line looks reasonable.

Scatter plots of the observed T_e over E , please see Fig. 4, show still a considerable variation of points from the ESR 32 m estimate compared with the earlier results of the tristatic UHF system (Jones et al., 1991). Possibly also overestimation of E occurs when there are two regions of high electric field for example north and south of the field-aligned ESR position. This would correspond to an occasional underestimation of σ_P^* .

Virtually connecting the red dots gives the curve corresponding to $E' = \sqrt{Bl_e/e}$ or $l_e = eE'^2/B$. At least below 110 km height this relation seems to be consistent with the data for high electric fields, $E \gtrsim 100 \text{ mVm}^{-1}$. The relation is certainly not valid for $E < E_{th}$. For intermediate field strengths, $E > E_{th}$, T_e seems to be below the one corresponding to the connected red dots. Also the previously published tristatic data do not seem to agree with a steep increase of T_e when E is moderately larger than E_{th} . Rather T_e seems to increase first roughly linearly with $E - E_{th}$, but then approach the values corresponding to $l_e = eE'^2/B$.

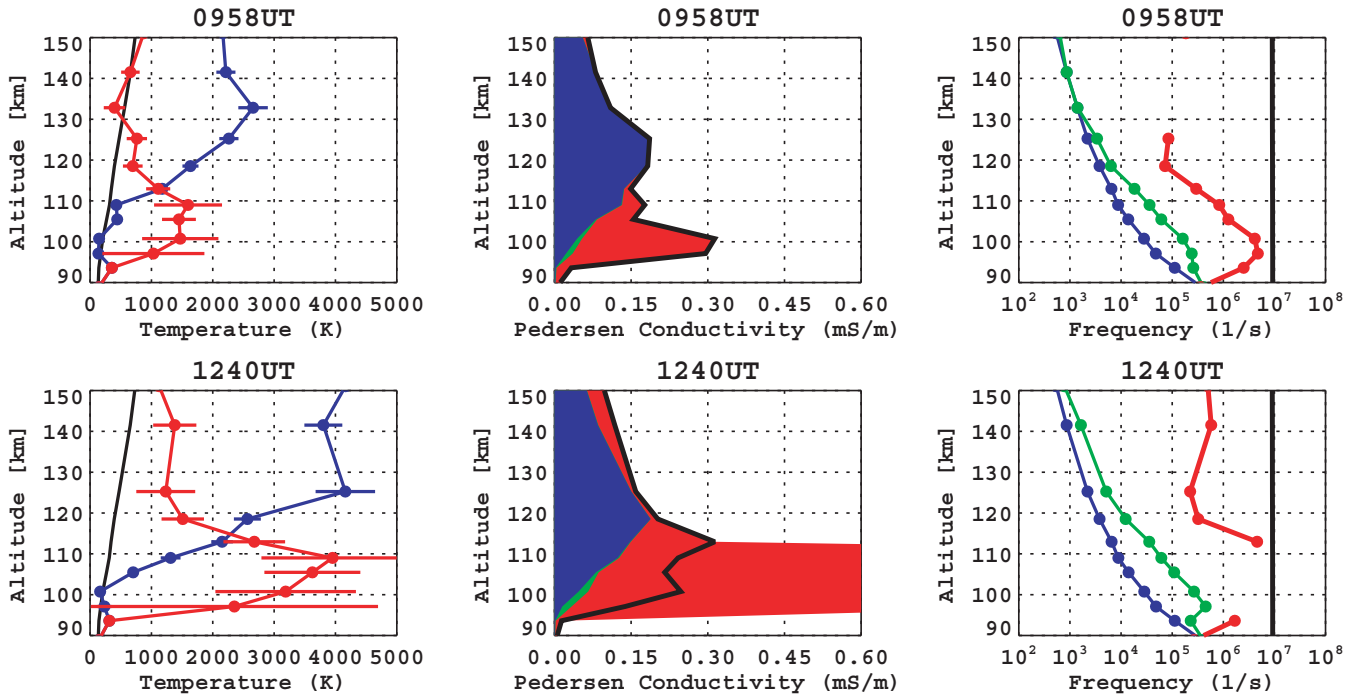


Fig. 3. Each column of plots shows from left to right altitude profiles of temperatures, Pedersen conductivity, and collision frequencies, respectively. In the temperature profiles T_e is plotted in red, T_i in blue, and T_n as black line. In the conductivity profiles the blue area shows the classical Pedersen conductivity calculated according to Brekke and Hall (1988), the (mostly hardly visible) green area the increase of σ_P due to enhanced T_e , and the red area the additional contribution from $\sigma_P^* = N_e l_e / E'^2$. The black line cuts through the red area whenever there is no corresponding real anomalous ν^* and shows the conductivity value corresponding to $\nu^* = \Omega_e$ instead. In the frequency profiles ν_{en} is plotted in blue, ν_{en} corrected for the observed T_e in green, ν^* in red, and Ω_e as a black line. The upper row shows a time of modest electron heating, the lower row one of very extreme heating.

We have also tested the heuristical hypothesis that the anomalous effect limits the velocity difference between ions and electrons to the ion sound velocity (analogue to Sudan, 1983, postulating that the phase velocity of irregularities is limited this way). However, this hypothesis turns out to require too strong heating, inconsistent with the scatter plots of the data shown in Fig. 4, and incompatible with the requirement of a real κ^* . The anomalous effect turns the mean electron velocity v_e into the direction anti-parallel to E and reduces the magnitude of v_e , but for increasing $E > E_{th}$ $|v_e - v_i|$ still increasingly exceeds the ion sound velocity.

Finally, the Pedersen conductances, i.e. height-integrated conductivities, without and with anomalous contribution are compared in Fig. 5. Using blindly the ESR 32 m estimates of E' and $\sigma_P^* = N_e l_e / E'^2$ would lead to sometimes enormous anomalous effects on the conductances, which we believe is not the case. After replacing the complex κ^* by $\kappa^* = 1$ and updating the anomalous Σ_P^* (blue dots in Fig. 5), an increase of the total Pedersen conductance by up to about 60% over the classical Σ_P due to strong E fields exciting electrojet irregularities remains.

3 Summary and conclusions

Incoherent scatter data at very high latitude on the day-side show sometimes extremely strong heating of the electrons in the electrojet, with temperatures up to about 4000 K at altitudes as low as 105 km. Also intense Joule heating of ions is observed simultaneously at higher altitudes. The heating is caused by dissipative Pedersen currents closing field-aligned current and so extracting and converting kinetic power from plasma convection in the near Earth space. While the ion Pedersen current is due to classical collisions between ions and neutrals, the electron current in the electrojet is affected by irregularities and plasma turbulence existing in the presence of high electric fields (Buchert et al., 2006). The effect can be parameterized by an anomalous collision frequency, that turns the mean electron velocity from the $E' \times B$ direction towards $-E'$, exactly like ion-electron collisions. A secondary effect of anomalous collisions is a retardation of $|v_e|$ compared to E'/B . Because of the with ν^* increasing retardation the strongest possible dissipation occurs for $\nu^* = \Omega_e$ at an angle of 45° between v_e and $-E'$. Then $E' = \sqrt{B l_e / e}$.

The anomalous Pedersen conductivity may be estimated from the electron density, the electron cooling rate, which is

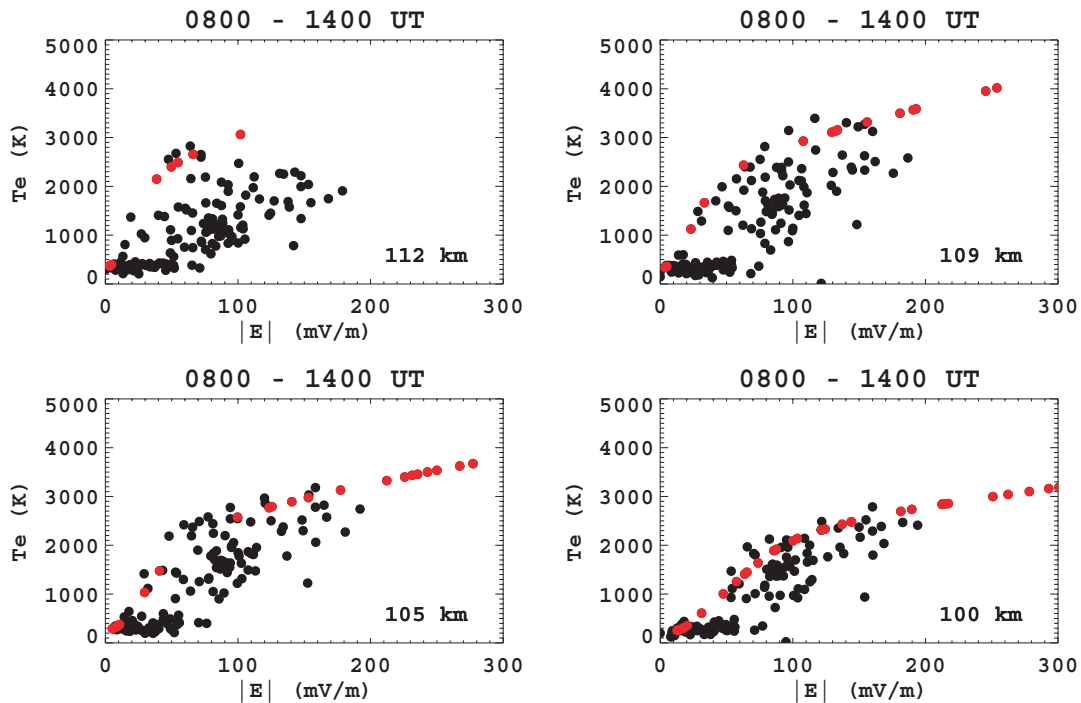


Fig. 4. Scatter plots of the observed T_e over estimated E at four different altitudes. Black dots are used for points when E is estimated from ESR 32 m line-of-sight observations, and red dots when $E' = \sqrt{B}I_e/e$ had been set because of complex κ^* , $A < 2$, and the ESR 32 m estimate of E obviously too low.

for $T_e > T_n$ a monotone function of $T_e - T_n$, and the electric field strength. Measurement errors, particularly underestimation of E when derived from spatially separated line-of-sight data, lead sometimes to too large values for σ_p^* , more than is possible even when $v^* = \Omega_e$. In these cases we have assumed that the real E corresponds to this highest possible dissipation, taking care of obvious overestimations of σ_p^* . After these corrections still increases of the effective Pedersen conductance by up to 60% relative to the classical values are derived.

Therefore the effective conductivities and also conductances do depend explicitly on the electric field for large strengths. High E , 100 mV m^{-1} and more, occur in the ionosphere at high latitudes both on the dayside as in this event and also in nightside auroral phenomena, like the westward traveling surge and Omega bands (Vanhamäki and Amm, 2007). If semi-empirical expressions for the dependency were available, they could potentially be used to improve techniques like KRM (Kamide et al., 1981, <http://gedas22.stelab.nagoya-u.ac.jp/>), AMIE (Richmond and Kamide, 1988), and CECS (Vanhamäki and Amm, 2007), where conductances and electric fields play a central role. More accurate data and a larger amount of data, but possibly also studies and simulations of the microphysics of the irregularities, should in the future result in a more quantitative understanding of the “non-linear” ionospheric Ohm’s law.

The Pedersen conductance dependence of E affects the reflection of Alfvén waves from the ionosphere, which is a widely used model for the investigation of pulsations and in dynamic simulations of the magnetosphere-ionosphere system. Probably the reflection process generates harmonics of pulsation frequencies similar to non-linearities in electrical oscillators.

Precipitation of energetic electrons can change the electron density in the E region, and therewith also conductances, relatively by much larger factors than we have derived for the irregularity effect. High electric fields and strong precipitation tend to occur simultaneously, but spatially hardly overlapping, i.e. strong flows are typically adjacent to auroral forms caused by precipitation. Due to the irregularity effect the conductances are enhanced also in the areas of strong flow, thus reducing conductance gradients at the edge of aurora but not eliminating them. Consequently the FAC contribution $\text{grad} \Sigma_P \cdot E$ probably gets overestimated when the irregularity effect is neglected. On the other hand, the contribution $\Sigma_P \text{div} E$ gets underestimated. FACs are a crucial parameter controlling particularly the onset of auroral breakups. Therefore the “non-linear” ionospheric response may to some extent influence onsets of auroral activity.

The altitude distribution of atmospheric heating by magnetospheric convection is significantly shifted towards lower heights when heating via electrojet irregularities is taken into account. In periods of strong E the heating rate actually

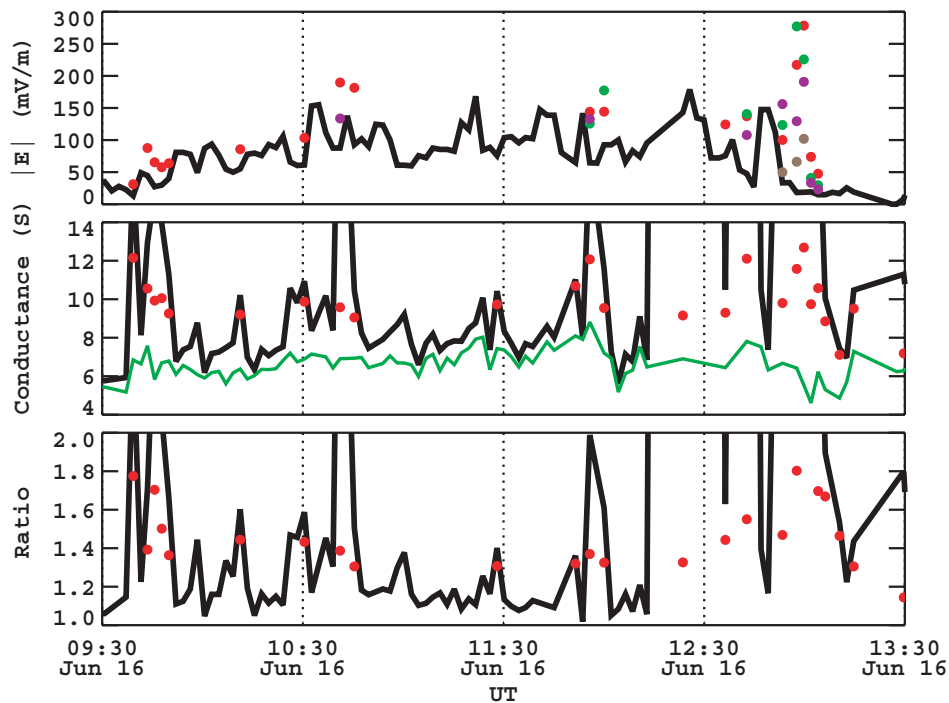


Fig. 5. From top to bottom electric field strength, Pedersen conductances, and the ratio of classical to total Pedersen are shown. When complex κ^* occurred then in the top panel dots show the value of $\sqrt{Bl_e/e}$ in red at 100, green at 105, purple at 109, and brown at 112 km height. In the middle panel the green curve shows Σ_P calculated according to Brekke and Hall (1988), the black curve $\Sigma_P + \Sigma_P^*$, and the red dots values after correcting Σ_P^* for underestimated E . The bottom panel shows the ratio $(\Sigma_P + \Sigma_P^*) / \Sigma_P$, red dots again values after correction for underestimated E .

peaks around 100–115 km (compare with Fig. 3), not near 125–130 km as the ion Pedersen current. The magnetic stress corresponding to the electron Pedersen current and its closure of field-aligned current transfers additional momentum from magnetospheric convection to the atmosphere. Joule heating and magnetospheric forcing are known to have effects on the neutral atmosphere dynamics. For example, the generation of gravity waves and a neutral fly wheel have been associated with auroral disturbances. However, these effects tend to diminish towards lower altitudes as the neutral inertia and energy density increases. The electron Pedersen current flows more than one neutral scale height below the ion Pedersen current, and the integrated effect of irregularities is smaller than the integrated ion current even for very high electric fields. This lets us believe that the effects of irregularities on atmospheric dynamics are probably small compared to those of ion drag and Joule heating. On the other hand, Nozawa and Brekke (1995) did notice that the neutral wind pattern on disturbed days is different from that at quiet days already at heights above 109 km, which is well below the altitude range of the ion current. A possible explanation is that the electron Pedersen current influences to some extent even the lower thermosphere. Future investigations should clarify more this question and the issues described above.

Acknowledgements. EISCAT is an International Association supported by Finland (SA), France (CNRS), Germany (MPG), Japan (NIPR), Norway (NFR), Sweden (VR) and the United Kingdom (PPARC).

Topical Editor K. Kauristie thanks O. Amm and M. Uspensky for their help in evaluating this paper.

References

- Bahcivan, H.: Plasma wave heating during extreme electric fields in the high-latitude E region, *Geophys. Res. Lett.*, 34, L15106, doi:10.1029/2006GL029236, 2007.
- Brekke, A. and Hall, C.: Auroral ionospheric quiet summer time conductances, *Ann. Geophys.*, 6, 361–375, 1988, <http://www.ann-geophys.net/6/361/1988/>.
- Buchert, S. C., Hagfors, T., and McKenzie, J. F.: Effect of electrojet irregularities on DC current flow, *J. Geophys. Res.*, 111, A02305, doi:10.1029/2004JA010788, 2006.
- Farley, D. T.: A plasma instability resulting in field-aligned irregularities in the ionosphere, *J. Geophys. Res.*, 68, 6083–6097, 1963.
- Jones, B., Williams, P. J. S., Schlegel, K., Robinson, T., and Häggström, I.: Interpretation of enhanced electron temperatures measured in the auroral E-region during the ERRRIS campaign, *Ann. Geophys.*, 9, 55–59, 1991, <http://www.ann-geophys.net/9/55/1991/>.

- Haldoupis, C.: Possible evidence for partial demagnetization of electrons in the auroral E-region plasma during electron gas heating, *Ann. Geophys.*, 12, 40–43, 1994, <http://www.ann-geophys.net/12/40/1994/>.
- Hedin, A. E.: Extension of the MSIS Thermosphere Model into the Middle and Lower Atmosphere, *J. Geophys. Res.*, 96, 1159–1172, 1991.
- Kamide, Y., Richmond, A. D., and Matsushita, S.: Estimation of Ionospheric Electric Fields, Ionospheric Currents, and Field-aligned Currents from Ground Magnetic Records, *J. Geophys. Res.*, 86, 801–813, 1981.
- Kelley, M. C.: The Earth's ionosphere: plasma physics and electrodynamics, Academic Press, San Diego, California, 34–41, 1989.
- Nozawa, S. and Brekke, A.: Studies of the E Region Neutral Wind in the Disturbed Auroral Ionosphere, *J. Geophys. Res.*, 100, 14 717–14 734, 1995.
- Opgenoorth, H. J., Häggström, I., Williams, P. J. S., and Jones, G. O. L.: Regions of strongly enhanced perpendicular electric fields adjacent to auroral arcs, *J. Atmos. Terr. Phys.*, 52, 449–458, 1990.
- Richmond, A. D. and Kamide, Y.: Mapping of Electrodynamic Features of the High-latitude Ionosphere from Localized Observations: Technique, *J. Geophys. Res.*, 93, 5741–5759, 1988.
- Robinson, T. R.: Toward a self-consistent non-linear theory of radar auroral backscatter, *J. Atmos. Terr. Phys.*, 48, 417–422, 1986.
- Schlegel, K. and St.-Maurice, J.-P.: Anomalous heating of the polar E region by unstable plasma waves: 1. Observations, *J. Geophys. Res.*, 86, 1447–1454, 1981.
- Schunk, R. W. and Nagy, A. F.: *Ionospheres*, Cambridge Univ. Press, New York, 258–264, 2000.
- Sudan, R. N.: Unified theory of type I and type II irregularities in the equatorial electrojet, *J. Geophys. Res.*, 88, 4853–4860, 1983.
- Vanhamäki, H. and Amm, O.: A new method to estimate ionospheric electric fields and currents using data from a local ground magnetometer network, *Ann. Geophys.*, 25, 1141–1156, 2007, <http://www.ann-geophys.net/25/1141/2007/>.
- Zhang, B.-C., Kamide, Y., Liu, R.-Y., Shinagawa, H., and Iwamasa, K.: A modeling study of ionospheric conductivities in the high-latitude electrojet regions, *J. Geophys. Res.*, 109, A04310, doi:10.1029/2003JA010181, 2004.